Effect of Compressive Stress on Fe Self-Diffusion in Nanocrystalline FeN(Zr) Thin Films

Sujoy Chakravarty,[1,3] Mukul Gupta,[2] Harald Schmidt,[1] Ajay Gupta[3]

[1]Institut für Metallurgie, TU Clausthal, D-38678 Clausthal-Zellerfeld, Germany
[2]UGC-DAE Consortium for Scientific Research, BARC, Mumbai, India
[3]UGC-DAE Consortium for Scientific Research, University Campus,
Khandwa Road, Indore, India

E-Mail: scha@tu-clausthal.de

Abstract. In the present work the effect of compressive stress on self-diffusion of Fe in nanocrystalline FeN(Zr) alloys has been investigated. Two different types of $Fe_{64}N_{26}Zr_{10}$ samples, one without applied stress and another with applied compressive stress of 42 GPa, were deposited under identical conditions using magnetron sputtering. The stress has been applied to the sample by bending the substrate during the deposition using a three point bending device. The self-diffusivities of Fe were determined by measuring the broadening of ^{57}Fe marker layers by Secondary Ion Mass Spectrometry after annealing at 443 K, 483 K and 523 K for 1 hour. The activation energy and pre-exponential factor for Fe diffusion is comparatively higher in the stressed sample. The higher activation energy might be due to the fact that the system transforms into a more dense state when compressive stress is applied.

1 Introduction

In recent years nanocrystalline metals and alloys have emerged as an important class of materials. The remarkable properties of these materials can be tailored by changing particle size, shape and morphology of nano-crystals [1-6]. Generally, this change is governed by atomic diffusion. Consequently, the knowledge of self-diffusion and of the underlying diffusion mechanisms is necessary to understand thermal stability, thermally induced microstructure changes and also stability against environment impact, which is important for technological application of these materials. Besides, a high fraction of atoms in nanocrystalline alloys is

present in grain boundaries (up to 40 %). Thus, they are also important systems for an understanding of grain boundary diffusion mechanisms.

Fe-N alloys are very important materials and extensive studies were done in order to understand their magnetic and mechanical properties as a function of chemical composition and microstructure [7-12]. However, a detailed investigation of self-diffusion in these materials is still lacking. Fe-N bonds are known to be one of the strongest covalent bonds in nature. Therefore, it is expected that vacancies exist as defects in amorphous FeN and diffusion should take place through a vacancy jump–mechanism. Recently, first diffusion studies were done on amorphous and nanocrystalline Fe-N thin films. It has been reported that the atomic diffusion is not similar to that of a vacancy jump mechanism. However, a diffusion mechanism is suggested where several atoms move collectively [13,14].

In case of materials are deposited in form of thin films on a substrate, large intrinsic strain and stress may be generated in the film. This stress may result from the lattice mismatch of the substrate and of the film and may be modified during annealing due to differences in the thermal expansion coefficients of the substrate and of the film (thermal stress). Another possibility is that it originates from the microstructure of the deposited film (intrinsic stresses) [15-17]. Intrinsic stress may occur at strained regions within a film during formation of grain-boundaries, dislocations, voids, impurities, etc [18]. This stress may significantly affect the physical properties of the films, including atomic diffusion. Since many devices which are used for applications are fabricated in the form of nm range thin films, an understanding of the effect of stress on atomic self-diffusion is extremely important.

In the present work, the effect of compressive stress on Fe self-diffusion in chemically homogeneous thin films of nanocrystalline Fe-N alloys has been investigated using Secondary Ion Mass Spectrometry (SIMS) depth profiling.

2   Sample Preparation

Chemically homogeneous thin films of composition $Fe_{64}N_{26}Zr_{10}$ were prepared by magnetron sputtering of composite FeZr targets on Si substrates. Small pieces of Zr rods were pasted on either $^{natural}Fe$ or ^{57}Fe targets in a symmetric way and the composite targets were sputtered alternately to prepare a chemically homogeneous film with the following structure

$$Si/^{natural}FeNZr/^{57}FeNZr/^{natural}FeNZr/^{57}FeNZr/^{natural}FeNZr.$$
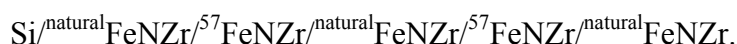
A mixture of nitrogen and argon gases (50 vol. % each) was used to sputter the composite target at a power of 50 W. The small amount of Zr (about 10 %) was essentially used to restrict the grain size of FeN, in order to produce a nanocrystalline structure. It is well known that the addition of a small amount of early transition metals in transition metal-metalloid systems results in inhibition of grain growth and the formation of a nanocrystalline structure [19]. The deposition of the film was carried out after obtaining a base pressure better than 1×10^{-6} mbar. During deposition, the pressure in the chamber was 5×10^{-3} mbar due to a gas flow of 30 cm^3/min.

During deposition the substrate was mounted on a specially designed three-point Si wafer bending device (Fig. 1). Thin Si wafers (300 ± 10) µm were used as a substrate in order to avoid breaking during bending. For bending, the Si wafer was fixed at both of the ends. The rotation of an asymmetric roller around the central axis bends the Si wafer at different bending heights varying between 0 and 5 mm. A pin lock system was incorporated in such a way that a release of bending by itself during deposition could be avoided. The bending was released after deposition, which results in an applied compressive stress on the film. The magni-

tude of applied compressive stress due to release of bending has been calculated using equation

$$\sigma = \frac{\left(\dfrac{E_{Si}}{1-v_{Si}}\right)T_{Si}^2}{6RT_f}$$

(1)

where $E_{Si}/(1-v_{Si})$ is the biaxial modulus of the silicon substrate which is equal to 180.5 GPa. E_{Si} is Young's modulus for Si and v_{Si} is Poisson's ratio for Si. T_{Si} is the thickness of the substrate, T_f is the thickness of the film, and R is the radius of curvature [20,21]. With the situation shown in Fig. 1, the radius can be written as

$$R = \frac{a^2 + b^2}{2b}$$

(2)

Combining eqns. (1) and (2), the value of stress was calculated.

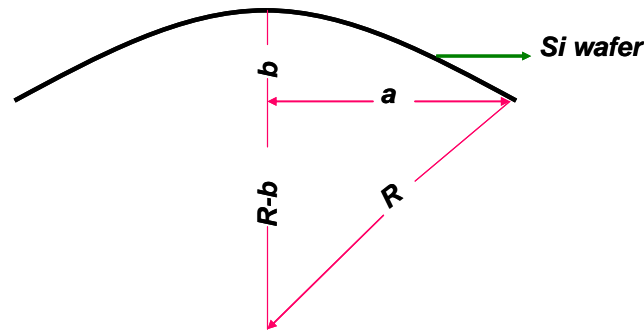**Fig. 1:** Schematic diagram of the bent Si wafer used for calculation of the radius of curvature.

The parameters used in the present case are $T_{Si} = (300 \pm 10)$ μm, $T_f = 400$ nm, $a = 40$ mm and $b = 5$ mm. The calculated value of stress is 42 GPa within error limits of 15 … 20%.

3 Structural Characterization

The thickness of the films was determined by measuring the crater formed during secondary ion mass spectrometry (SIMS) depth profiling using a mechanical profilometer (TENCOR). The average thickness of the film is about 400 nm and the structure of the film is

Si/[nat.]FeNZr(120nm)/[57]FeNZr(20nm)/[nat.]FeNZr(120nm)/[57]FeNZr(20nm)/[nat.]FeNZr(120m).

    The chemical composition of the film was determined using X-ray photoelectron spectroscopy (XPS) to be $Fe_{64}N_{26}Zr_{10}$. Conversion electron Mössbauer spectra (CEMS) of the sample consist of a broad doublet. The spectrum has been fitted with two doublets and two singlets in accordance with literature results on iron nitride [22]. The fitted parameters are very close to those of crystalline $Fe_{60}N_{40}$ [22]. This result suggests that the small amount of Zr added for inhibiting the grain growth is not located inside the FeN crystals, but it is probably present at the grain-boundary regions. Annealing up to 573 K does not result in any significant change

in the hyperfine field parameters, indicating that the local environment of Fe remains unchanged up to 573 K. Annealing at 673 K results in a qualitative change in the shape of the Mössbauer spectrum and hyperfine field parameters. Thus, the Mössbauer measurement suggests that the as deposited nanocrystalline phase is stable up to 573 K.

Fig. 2 a) shows the X-ray diffraction (XRD) pattern of the film after annealing at different temperatures for a period of 30 min each. The diffraction pattern of the pristine sample exhibits a broad peak at a scattering angle of about 58 °, corresponding to the γ-iron nitride phase. The crystallite size as obtained from the width of the diffraction peak using the Scherrer formula [23,24] is about 2 - 3 nm. Thermal annealing up to 573 K shows only minor variations
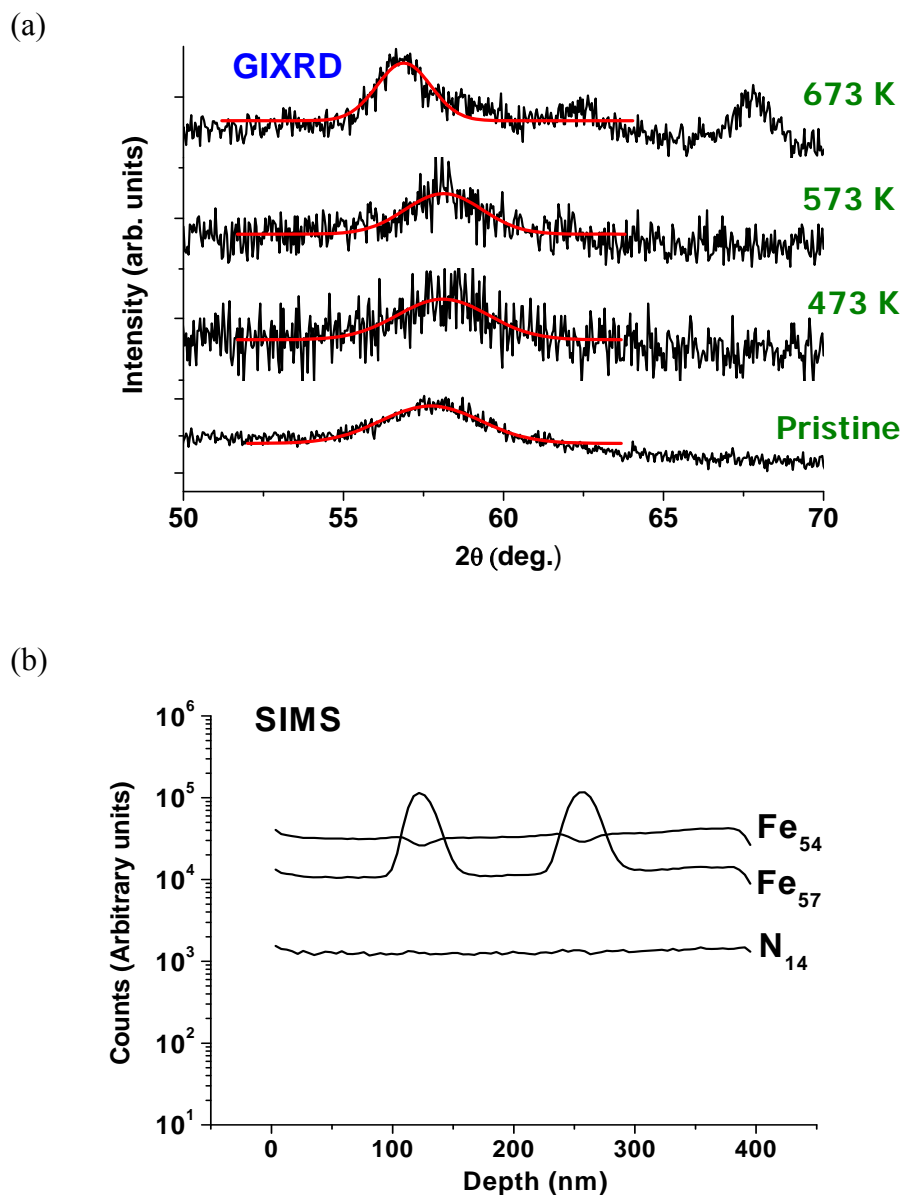

Fig. 2: XRD pattern of the films for 0.5 h anneals at different temperatures. The red curves represents Gaussian fits to the Bragg peaks in order to attain the FWHM. (b) SIMS depth profile of ^{54}Fe, ^{57}Fe and ^{14}N in the as deposited film.

in the XRD pattern. However, annealing above 573 K results in appearance of an additional peak, suggesting the occurrence of a phase transformation. This is also supported by the CEMS measurements. Furthermore, annealing up to 573 K does not cause any change in grain size.

In conclusion, CEMS, XRD and XPS measurements suggest that the microstructure of the film consists of nanograins of γ-iron nitride with additional segregation of Zr at grain boundaries. The chemical composition of the nanograins is $Fe_{60}N_{40}$, as obtained from CEMS.

Fig. 2 b) shows the SIMS depth profile of ^{57}Fe, ^{54}Fe and ^{14}N in the as deposited film. The ^{57}Fe signal shows two peaks of equal intensity at the position of the two marker layers, whereas ^{54}Fe shows corresponding dips at those two positions. The intensity of the nitrogen profile is constant throughout the depth, indicating a constant nitrogen concentration. The ^{57}Fe depth profiles are somewhat skewed towards higher sputtering time. This asymmetry in the depth profiles is due to intermixing induced by the 5 keV O^+ primary ions used for sputtering. A correction of this profile broadening was done using a procedure described in literature, see Refs. [13,25,26].

4 Diffusion Measurements

For diffusion measurements samples without applied stress and samples with an applied stress of 42 GPa are annealed simultaneously for 1 hour at 443 K, 483 K and 523 K, respectively. The diffusion annealing of the samples was performed in a vacuum furnace with a base vacuum better than 10^{-6} mbar. The self-diffusivity of Fe was calculated from the broadening of the ^{57}Fe concentration depth profiles, measured by a CAMECA IMS 3f secondary ion mass spectrometer. The primary ions used for sputtering were O^+ ions of energy 5 keV and the ion current was about 50 nA. A typical broadening of ^{57}Fe depth profile after annealing at 483 K for 1 hour is shown in Fig. 3. The profiles have already been corrected for the intermixing effect of the O^+ primary ions.
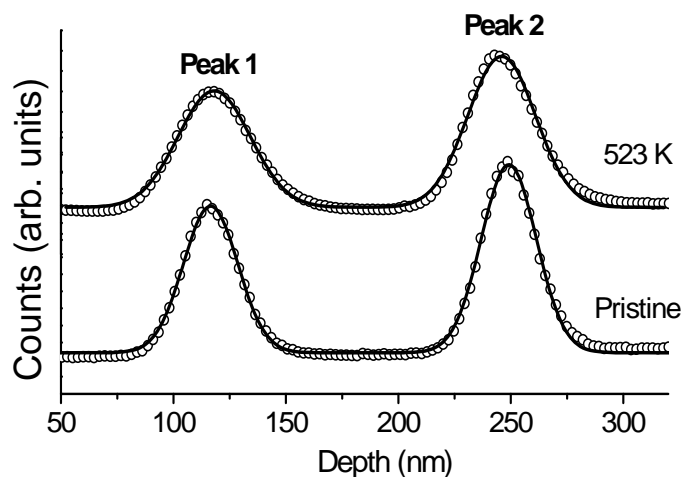

Fig. 3: Diffusion broadening of the ^{57}Fe SIMS depth profile after annealing at 523 K for 1 hour.

In the present case, the tracer concentration of ^{57}Fe as a function of penetration depth x is given by [27]

$$c(x,t) = \frac{const.}{\sigma_t \sqrt{2\pi}} \exp[-(x-x_0)^2 / 2\sigma_t^2], \tag{3}$$
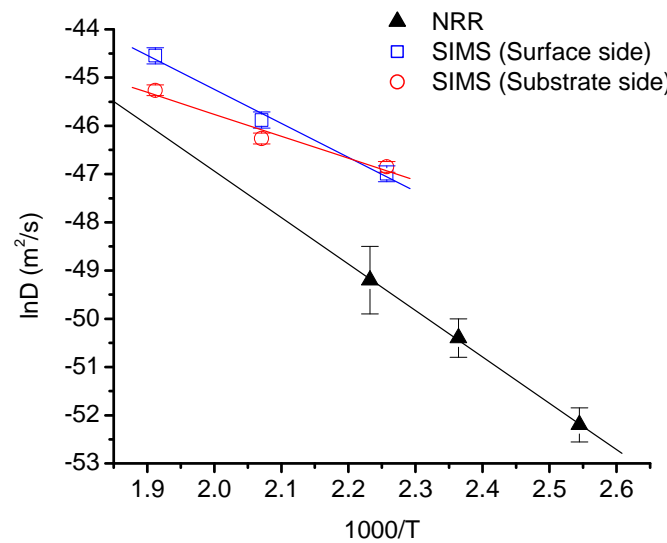
Fig. 5: Arrhenius plot of the diffusion coefficients with and without applied stress as calculated from the broadening of ^{57}Fe marker layer at (a) the surface side (peak 1) and (b) the substrate side (peak 2).

where x_0 is the position of the isotopic marker layer. Accordingly, the diffusion coefficients were calculated using the equation

$$\langle D \rangle (t) = \frac{\sigma_t^2 - \sigma_0^2}{2t} \quad , \tag{4}$$

where D is the diffusion coefficient and σ_0 and σ_t are the standard deviations of Gaussian depth profiles before annealing and after annealing the sample for the time period t, respectively [26].

The diffusivities plotted as a function of temperature, T, were used to calculate activation energy, q, and pre-exponential factor, D_0, using the Arrhenius equation

$$D = D_0 \exp(-q / k_B T) \tag{5}$$

The results for $\ln(D_0)$ and q obtained in this study are given in Table 1. Fig. 4 shows the plot of lnD vs 1000/T for Fe self-diffusion in the sample without stress. For comparison, recently published data on Fe self-diffusion in nanocrystalline FeN(Zr) done by nuclear resonance reflectivity (NRR) [14] has also been included in the graph.

Table. 1 $\ln(D_0)$ and q for diffusion in nanocrystalline $Fe_{64}N_{26}Zr_{10}$.

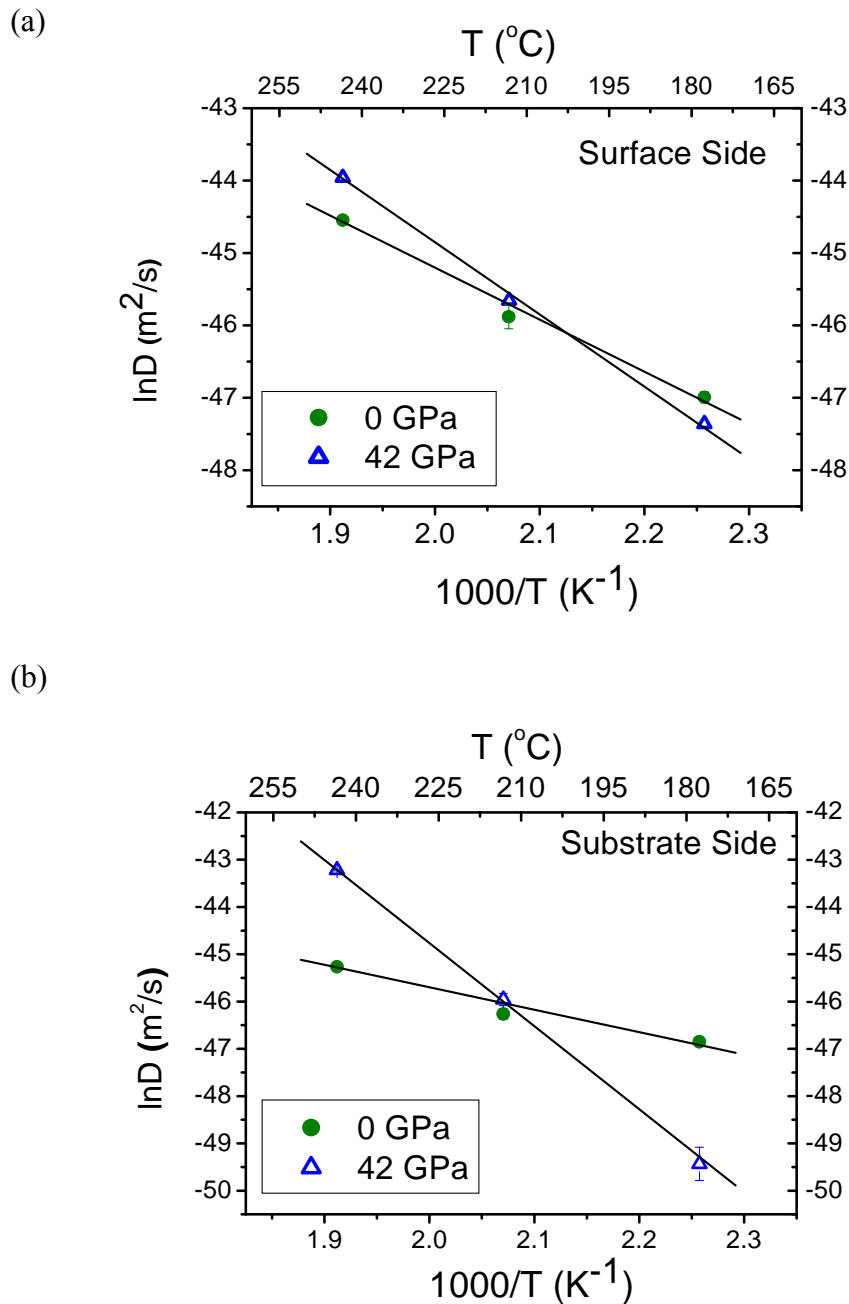| position of the marker layer	0 GPa		42 GPa	
	$\ln(D_0$ $s \cdot m^{-2})$	q (eV)	$\ln(D_0$ $s \cdot m^{-2})$	q (eV)
surface side (peak 1)	-31 ± 2	0.6 ± 0.1	-25 ± 2	0.9 ± 0.1
substrate side (peak 2)	-36 ± 1	0.4 ± 0.1	-9.6 ± 0.7	1.5 ± 0.1

(a)

(b)

Fig. 5: Arrhenius plot of the diffusion coefficients with and without applied stress as calculated from the broadening of [57]Fe marker layer at (a) the surface side (peak 1) and (b) the substrate side (peak 2).

Fig. 5 a) and b) show the plot of $\ln D$ vs $1000/T$ for the samples with and without stress as calculated from the marker layer broadening at the surface side (peak 1) and the substrate side (peak 2).

5 Discussion

It is obvious from Fig. 4 that the diffusivities in the stress free case as measured by SIMS do not coincide with the interpolated data as measured by NRR. At a temperature of 443 K the

diffusivity examined by SIMS is larger by a factor of 50 compared to the diffusivity measured by NRR. The reason for that is unclear at the moment and needs further investigation. Possible structural relaxation processes which might lead to a time dependence of diffusion can be excluded as a reason, since the annealing times were chosen in a way that a well relaxed state is present for 1 h of annealing at the temperatures investigated (see Ref. [14]). However, one has to recognize that two completely different methods were used to determine diffusivities in the present case. The first method (SIMS) is a very established method, while the second (NRR) is a relatively new method, whose application for diffusivity determination is still not sufficiently tested and has to be investigated in more detail. Further, the samples used for the two types of measurements are produced in the same way and have the same chemical composition, however, the present sample has only two enriched layers of ^{57}Fe while the sample for the NRR measurements is an isotope multilayer with ten ^{57}Fe layers. With NRR the average modification of the whole isotope multilayer is detected, while for SIMS the broadening of a special peak is observed, meaning that the difference might be caused by the fact that diffusivities obtained from local and integral data are compared.

A hint that the diffusivity might be dependent on the distance of the marker layer from the surface is supported by the observation that the diffusivities (especially at 523 K) and the values of q and D_0 for the surface side peak and the substrate side peak is slightly different (see Fig. 4 and Table 1). This difference might be due to a possible influence of the close by surface, where a small oxide layer might act as source of point defects diffusing in and influencing the Fe diffusion. On the other side, the Si-film interface might also act as a sink of point defects. However, the absolute effect is very small and only pronounced at 523 K (about a factor of 2). Consequently, more detailed measurements have to reveal whether a significant physical effect is acting here.

From Fig. 5 it can be observed that the applied stress has a significant, but unusual effect on the self-diffusivity of Fe. First, it is obvious that the effect at the substrate side is significantly more pronounced than the effect the surface side. This difference can be explained due to a variation of the compressive stress as a function of depth. At the substrate side the stress is higher than at the surface side. We assume that a substantial relaxation of stress, which is induced by the lattice mismatch of film and substrate, takes place in a region more close to the surface, leading to a decrease of the stress with increasing distance from the substrate.

It is further observed that the activation energy and the pre-exponential factor for Fe self-diffusion in nanocrystalline FeN(Zr) increases with applied compressive stress. We explain this by the fact that the stress modifies the structural state of the sample, meaning the stressed sample is in a more dense state than the unstressed sample. Structural defects like free volumes or vacancies are reduced and a more dense state is formed. Within this state it is more difficult for the atoms to diffuse and consequently a higher activation energy is necessary.

These findings are supported by a recent study on Fe self-diffusion in nanocrystalline FeZr thin films. There, a decrease in diffusivity has also been observed with applied compressive stress [28]. However, as far as the authors know the effect of applied stress on atomic diffusivity in structurally relaxed nanocrystalline systems has not been studied in detail so far. Therefore, the present study will give some preliminary overview on this point and leaves some open questions which need further detailed investigations.

6 Conclusion

In conclusion, the effect of compressive stress on self-diffusion of Fe in a nanocrystalline FeN(Zr) alloy has been investigated using SIMS depth profiling technique. It was observed that the activation energy and pre-exponential factor for Fe diffusion is comparatively higher

in the stressed sample. The higher activation energy might be due to the fact that the system transforms into a more dense state when compressive stress is applied.

References

[1]   A. Dunlop, G. Jaskierowicz, G. Rizza, and M. Kopcewicz, Phys. Rev. Lett. 90, 015503 (2003)
[2]   P. G. Debenedetti and F. H. Stillinger, Nature (London) 410, 259 (2001).
[3]   C. A. Angell, K. L. Ngai, G. B. mcKenna, P. F. McMillan, and S. Martin, J. Appl. Phys. 88, 3113 (2000).
[4]   M. E. McHenry, M. A. Willard, and D. E. Laughlin, Prog. Mater. Sci. 44, 291 (1999).
[5]   H. Tanimoto, P. Farber, R. Würschum, R. Z. Valiev, and H. E. Schaefer, Nanostruct. Mater. 12, 681 (1999).
[6]   A. Grandjean, P. Blanchard, and Y. Limoge, Phys. Rev. Lett. 78, 697 (1997).
[7]   X. Wang, W. T. Zheng, H. W. Tian, S. S. Yu, W. Xu, S. H. Meng, X. D. He, J. C. Han, C. Q. Sun, and B. K. Tay, App. Surf. Sci. 220, 30 (2003).
[8]   P. Preito, F. J. Palomares, J. M. Gonzalez, R. Pérez-Casero, and J. M. Sanz, Surface and Interface Analysis 38, 392 (2006).
[9]   X. Wang, W. T. Zheng, L. J. Gao, L. Wei, W. Guo, Y. B. Bai, W. D. Fei, S. H. Meng, X. D. He, and J. C. Han, J. Vac. Sci. Technol. A 21(4), 983 (2003).
[10] H. Naganuma, R. Nakatani, Y. Endo, Y. Kawamura, and M. Yamamoto, Japanese Journal of Appl. Phys. 43 (7A), 4166 (2004).
[11] J. F. Bobo, H. Chatbi, M. Vergnat, L. Hennet, O. Lenoble, Ph. Bauer, and M. Piecuch, J. Appl. Phys.77(10), 5309 (1995).
[12] R. Dubey, A. Gupta, and J. C. Pivin, Phys. Rev. B. 74, 214110 (2006).
[13] M. Gupta, A. Gupta, S. Rajagopalan, and A. K. Tyagi, Phys. Rev. B. 65, 214204 (2002).
[14] A. Gupta, M. Gupta, S. Chakravarty, R. Rüffer, H. C. Wille, and O. Leupold, Phys. Rev. B. 72, 014207 (2005).
[15] R. Abermann and R. Koch, Thin Solid Films 129, 71 (1985).
[16] A. L. Shull and F. Spaepen, J. Appl. Phys. 80, 6243 (1996).
[17] J. Floro, S. J. Hearne, J. A. Hunter, P. Kotula, E. Chason, S. C. Seel, and C. V. Thompson, J. Appl. Phys. 89, 4886 (2001).
[18] R. Koch, J. Phys.: Condens. Matter 6, 9519 (1994)
[19] M. E. McHenry, M. A. Willard, and D. E. Laughlin, Prog. Mater. Sci. 44, 291 (1999).
[20] G. G. Stoney, Proc. R. Soc. London, Ser. A 82, 172 (1909).
[21] J. Chen and I. D. Wolf, Semicond. Sci. Technol. 18, 261 (2003).
[22] L. Rissanen, M. Neubauer, K. P. Lieb, and P. Schaaf, J. Alloys Compd. 274, 74 (1998)
[23] P. Scherrer, Nachr. Königl. Gesell. Wiss. Göttingen 98 (1918).
[24] Mario Birkholz, Thin Film Analysis by X-Ray Scattering (Wiley-Vch Verlag Gmbh 2006), p. 110.
[25] G. Brebee, R. Seguin, C. Sella, J. Bevenot, and J. C. Martin, Acta Metall. 28, 327 (1980).
[26] Y. Loirat, J. L. Boequet, and Y. Limoge, J. Non-Cryst. Solids 265, 252 (2000).
[27] P. G. Shewmon, Diffusion in solids (McGraw-Hill, New York, 1963), p. 7.
[28] M. Gupta, A. Gupta, S. Chakravarty, R. Gupta, and T. Gutberlet, Phys. Rev. B 74, 104203 (2006).